

# Kernel Polynomial Method and Spectral Density Estimation

Jabed Umar\*

*School of Physical Sciences, National Institute of Science Education and Research, HBNI, Jatni-752050, India*

(Dated: April 22, 2024)

The Kernel Polynomial Method (KPM) is a technique used to approximate functions as finite-order polynomials. In this project, KPM is applied to approximate the density of states (DoS) in graphene and 3D semimetal systems. To achieve this, a tight-binding Hamiltonian for graphene is derived using the Kwant Python package, facilitating the implementation of KPM. One of the notable advantages of KPM is its ability to handle large system sizes effectively, thanks to its statistical approximation approach, which enhances accuracy with increasing system sizes. The project delves into the complete algorithm and mathematical foundations of KPM. It also explores how different parameters within KPM affect convergence criteria, thus influencing the accuracy of the approximations. Furthermore, the project investigates the density of states (DoS) in Weyl Nodal Loop semimetals. It demonstrates that by increasing the strength of disorder, a finite DoS can be achieved at energy  $(E) = 0$ , highlighting an intriguing aspect of these materials.

## I. INTRODUCTION

Physics grapples with the complexity of solving intricate equations governing microscopic systems, necessitating advanced approximations and analytical tools. Recent research has pivoted towards understanding complex systems with numerous interacting components, highlighting the limitations of traditional analytical methods. This shift has spurred the adoption of numerical approaches, leveraging advancements in computer power to enable feasible direct simulations of microscopic equations for larger systems. Consequently, developing and refining efficient algorithms have become paramount, driving significant research efforts in theoretical physics. These efforts aim to bridge the gap between fundamental theories and practical simulations, advancing our understanding of diverse phenomena in the realm of complex systems and materials.

On a microscopic scale, the behaviour of physical systems, including thermodynamics and responses to external factors, hinges on the distribution of eigenvalues and properties of eigenfunctions from a Hamiltonian operator—a Hermitian matrix of finite dimension  $D^2$ . Even for a moderate number of particles, lattice sites, or grid points,  $D$  can grow significantly, making the task of calculating all eigenvalues and eigenvectors daunting. The memory required scales as  $D^2$  while the number of operations and computation time scales as  $D^3$ , making it intractable for large  $D$ . This limits the system size that traditional approaches can effectively study, with the current practical limit around  $D \approx 10^5$  for dense matrices and slightly better for sparse matrices.

In this project, we explore numerical Chebyshev expan-

sion and the kernel polynomial method (KPM), which offer viable alternatives to traditional approaches. These iterative methods focus on multiplying the matrix with a small vector set, significantly reducing resource consumption. Resource scaling is linear with  $D$  for sparse matrices, while for others, it's around  $D^2$ . By constructing the matrix dynamically rather than storing it, we can handle dimensions up to  $D \approx 10^9$  or higher, vastly expanding the scope of systems we can study effectively.

The kernel polynomial method (KPM) is utilized for computing high-resolution spectral densities, static thermodynamic quantities, and zero-temperature dynamical correlations [1 - 5]. More recently, it has been expanded to include dynamical correlation functions at finite temperatures. KPM is a versatile tool for tackling large matrix problems and can be integrated as a fundamental element in more complex numerical techniques. It relies on statistical approximation, ensuring convergence but without a definite guarantee of the convergence rate.

The project is initially focused on Chebyshev polynomials and their role within the Kernel Polynomial Method (KPM) algorithm, detailed in **Section II**. Then, **Section III** delves into exploring Weyl Nodal Loop semimetals. The discussion concludes by addressing other methods and potential future applications of the KPM in **Section IV**. In the **Section V**, there's a brief but significant mention of the Density of States (DoS) and its relevance, Chebyshev polynomials and their properties and the DoS calculation for graphene by varying different parameters of KPM.

---

\* jabed.umar@niser.ac.in

## II. THE KERNEL POLYNOMIAL METHOD

### A. Chebyshev expansion and rescaling

The sole thing of KPM is the Chebyshev polynomial. By using the Chebyshev polynomial, a function  $f(x)$  can be written as

$$f(x) = \frac{1}{\pi\sqrt{1-x^2}}(\mu_0 + 2\sum_{n=1}^{\infty}\mu_n T_n(x)) \quad (1)$$

Where  $\mu_n = \int_{-1}^1 f(x)T_n(x)dx$ .

The important point is the function takes value in the interval  $[-1,1]$ . But our Hamiltonian has energy from  $E_{min}$  to  $E_{max}$ . So we need to rescale the energy values to make all of them in the interval  $[-1, 1]$ ; the rescaled eigenvalues  $\tilde{E}$  will have to be in the range  $-1 \leq \tilde{E} \leq 1$  (strict inequality can be used to avoid stability problems) To achieve this, the following scaling will be done [2, 3]:

$$\tilde{E} = \frac{E - b}{a} \implies \tilde{H} = \frac{H - bI}{a} \quad (2)$$

With the scaling factors  $a = \frac{E_{max} - E_{min}}{2 - \epsilon}$  and  $b = \frac{E_{max} + E_{min}}{2}$ , where  $\epsilon$  is a small number (typically set to 0.05 in applications like **Kwant** [8]) employed for convergence or stability problems that arise if the spectrum includes or exceeds the boundaries of the interval  $[-1,1]$ .

### B. Calculation of moments

Calculating the moment is crucial to expanding a function in the Chebyshev polynomial, eventually giving us DoS. The moment is defined as

$$\mu_n = \langle \beta | T_n(\tilde{H}) | \alpha \rangle = \langle \beta | \alpha_n \rangle \quad (3)$$

Where  $\alpha$  and  $\beta$  are the states of  $\tilde{H}$ .  $\mu_n$  and  $|\alpha_n\rangle$  can be calculated recursively using the recurrence relations of the Chebyshev polynomial. We have

$$T_0(x) = 1, T_1(x) = x, T_{m+1}(x) = 2xT_m(x) - T_{m-1}(x)$$

which will give us

$$|\alpha_0\rangle = |\alpha\rangle, |\alpha_1\rangle = \tilde{H}|\alpha\rangle, |\alpha_n\rangle = 2\tilde{H}|\alpha_{n-1}\rangle - |\alpha_{n-2}\rangle$$

By imposing the constraint of  $\tilde{H} = \tilde{H}^\dagger$  [2], we can get

$$\mu_{2n} = 2\langle \alpha_n | \alpha_n \rangle - \mu_0, \mu_{2n+1} = 2\langle \alpha_{n+1} | \alpha_n \rangle - \mu_1.$$

Let's expand the DoS in terms of  $\mu$ . The DoS of  $\tilde{H}$  is given by

$$\tilde{\rho}(\tilde{E}) = \frac{1}{D} \sum_{k=0}^{D-1} \delta(\tilde{E} - \tilde{E}_k) \quad (4)$$

Since we are trying to expand the DoS in terms of moments, so

$$\mu_n = \int_{-1}^1 \tilde{\rho}(\tilde{E}) T_n(\tilde{E}) d\tilde{E} = \frac{1}{D} Tr(T_n(\tilde{H})) \quad (5)$$

So, ultimately, the moment calculation is reduced to a trace estimation problem.

### C. Statistical approximation

In the last section we get that,  $\mu_n$  as the trace of  $T_n(\tilde{H})$ . To estimate this trace without requiring all the eigenvectors, we employ stochastic trace estimation:

$$\mu_n = \frac{1}{D} Tr(T_n(\tilde{H})) \approx \frac{1}{RD} \sum_{r=1}^R \langle r | T_n(\tilde{H}) | r \rangle \quad (6)$$

In this equation,  $|r\rangle$  represents a randomly selected state, allowing us to approximate the trace using only a random set of states. This approach is advantageous when  $R \ll D$ , as it eliminates the need to calculate the entire trace. Furthermore, we can utilize the recursive relation derived earlier to compute all the moments efficiently.

To choose a random vector, we start with a set of random variables  $\zeta_{ri} \in \mathbb{C}$  and a basis  $|i\rangle$  of dimension  $D$ . We construct the random vector  $|r\rangle$  as follows:

$$|r\rangle = \sum_{i=0}^{D-1} \zeta_{ri} |i\rangle \quad (7)$$

Here, the double index  $i, r$  of  $\zeta_{ri}$  signifies that a distinct  $\zeta_{ri}$  is selected for each vector in the basis and for each random vector. The  $\zeta_{ri}$  can be drawn from a distribution with specific statistical properties:

1.  $\lim_{N \rightarrow \infty} \frac{1}{N} \sum_{i=1}^N \zeta_{ri} \equiv \langle \langle \zeta_{ri} \rangle \rangle = 0$
2.  $\langle \langle \zeta_{ri} \zeta_{r'j} \rangle \rangle = 0$
3.  $\langle \langle \zeta_{ri}^* \zeta_{r'j} \rangle \rangle = \delta_{rr'} \delta_{ij}$

Various distributions, like Gaussian or uniform distributions, can meet these conditions.

Since  $|r\rangle$  is random, the variance of  $\theta (= \frac{1}{R} \sum_{r=1}^R \langle r | T_n(\tilde{H}) | r \rangle)$  could still be very high. Thankfully, this is not the case. The variance of  $\theta$  is given by:  $(\delta\theta)^2 = \langle \langle \theta^2 \rangle \rangle - \langle \langle \theta \rangle \rangle^2$ . Upon simplifying all the terms, we will get

$$(\delta\theta)^2 = \frac{1}{R} [Tr(T_n(\tilde{H})^2) + (\langle \langle |\zeta_{ri}|^4 \rangle \rangle - 2) \sum_{j=0}^{D-1} T_n(\tilde{H})_{jj}^2]$$

The trace of a matrix is usually  $\mathcal{O}(D)$ , as it is proportional to the dimension of the matrix. Therefore, the relative error  $\frac{\delta\theta}{\theta}$  will usually be  $\mathcal{O}(\frac{1}{\sqrt{RD}})$ . As a result, the number of random states that need to be evaluated decreases for a larger matrix.

Also, since the fluctuations depend on  $\langle \langle |\zeta_{ri}|^4 \rangle \rangle$ , the  $\zeta_{ri}$  should ideally be chosen such that this term is

as close as possible to 1 (can never be less than 1 because of property 3). We mostly use two choices of  $\zeta_{ri}$ ; their advantages and disadvantages are discussed below.

1. When  $\zeta_{ri} = e^{i\phi}$ ,  $\phi \in [0, 2\pi]$  a random phase, then  $(\delta\theta)^2$  will be influenced by both the trace term and last term unless we work in the eigenbasis of  $T_n(\tilde{H})$ .
2. When  $\zeta_{ri}$  is from Gaussian distribution, then  $\langle\langle |\zeta_{ri}|^4 \rangle\rangle = 2$  so  $(\delta\theta)^2$  will only be influenced by trace term. Since the trace term is independent of the basis, the variance will be independent of the basis. So, this is also a useful choice.

#### D. Kernel improvement

We turn to Chebyshev polynomials to expand functions  $f(x)$ , yet practically, we can't extend these expansions to infinite orders  $\mu$ . This limitation leads us to the classic problem of approximation theory. Our goal then becomes finding the best uniform approximation to  $f(x)$  using a polynomial of a specified maximum degree, typically denoted as  $N$  moments  $\mu_n$ . Experience has taught us that a straightforward truncation of an infinite series yields poor accuracy and introduces fluctuations, commonly referred to as **Gibbs oscillations**. These oscillations occur prominently near points where  $f(x)$  lacks continuous differentiability. A critical consideration in this context is the DoS, represented by a collection of delta functions, which necessitates caution regarding Gibbs oscillations [2].

To circumvent this issue, we rescale the moments  $\mu_n \rightarrow g_n \mu_n$ , where  $g_n$  is called the kernel. As  $N \rightarrow \infty$ , this transformation yields:

$$|f(x) - f_{KPM}(x)| \rightarrow 0$$

In the realm of Mathematics, there has been extensive discourse regarding the selection of an appropriate kernel, with a comprehensive discussion available in [3]. Notably, the '**Jackson kernel**' has emerged as a favourable choice due to its characteristics: it doesn't have free parameters, remains positive throughout the entire region, and exhibits convergence of  $\mathcal{O}(1/N)$ , indicating rapid convergence as  $N$  increases. The Jackson Kernel is defined as

$$g_n = \frac{1}{N+1} \left[ (N-n+1) \cos \frac{\pi n}{N+1} + \sin \frac{\pi n}{N+1} \cos \frac{\pi}{N+1} \right]$$

#### E. Cosine transformation and rescaling

After covering the theory of Chebyshev expansion, moment calculations, and different kernel approximations, let's focus on the practical aspects of implementing KPM. Specifically, we'll discuss the reconstruction

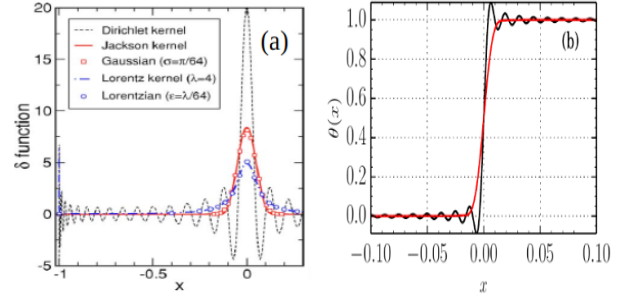


Figure 1. (a) Fitting of  $\delta$  function with different kernel. (b) Fitting of  $\theta$  function with (red) kernel and without (black) kernel. Image taken from [3] and [5]

of the expanded function  $f(x)$  from its moments  $\mu_n$ . When we have a finite number  $N$  of coefficients  $\mu_n$ , we discretize  $x$  by selecting certain points  $x_k$  at which the expansion will be evaluated. Consequently, our function  $f(x_k)$  will be represented as follows:

$$f(x_k) = \frac{1}{\pi \sqrt{1-x_k^2}} \left( g_0 \mu_0 + 2 \sum_{n=1}^{N-1} g_n \mu_n T_n(x_k) \right) \quad (8)$$

For a set  $x_k$  containing  $\tilde{N}$  points, these summations would require the order of  $N\tilde{N}$  operations. We choose the data points  $x_k$  as Chebyshev Nodes, which are useful for numerical analysis and are defined as

$$x_k = \cos \frac{\pi(k+1/2)}{\tilde{N}} \quad \text{for } k = 0, 1, \dots, \tilde{N}-1 \quad (9)$$

$N$  and  $\tilde{N}$  need not be the same, and the usual choice is  $\tilde{N} \geq N$  and a reasonable choice is  $\tilde{N} = 2N$ . We can return our desired  $f(x_k)$  by using the discrete cosine transformation.

$$\begin{aligned} \gamma_k &= \sqrt{1-x_k^2} f(x_k) = g_0 \mu_0 + 2 \sum_{n=1}^{N-1} g_n \mu_n T_n(x_k) \\ &= g_0 \mu_0 + 2 \sum_{n=1}^{N-1} g_n \mu_n \cos \left( n \left( \arccos \left( \cos \left( \frac{\pi(k+1/2)}{\tilde{N}} \right) \right) \right) \right) \\ &= g_0 \mu_0 + 2 \sum_{n=1}^{N-1} g_n \mu_n \cos \left( \frac{\pi(k+1/2)}{\tilde{N}} \right) \end{aligned} \quad (10)$$

So,  $\gamma_k$ , the discrete cosine transform of the moments  $\mu_n$ , a calculation that can be performed efficiently and represents a significant improvement over direct summation.

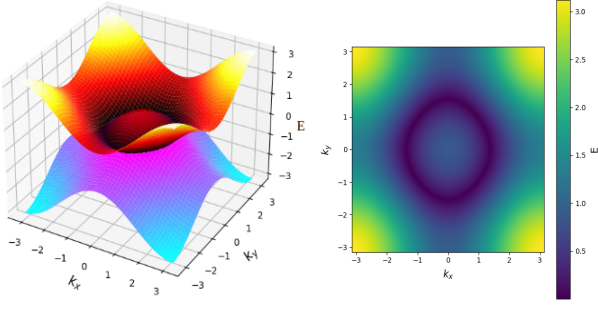


Figure 2. Left panel: energy bands for  $k_z = 0$  and  $k_x, k_y \in [\pi, \pi]$ . We have set  $t_x = 1.1$ ,  $t_y = 0.9$ ,  $t_2 = 0.8$  and  $m = 2.12$  (These parameters are used for all the plots). Right panel: top view of the higher energy band. There is a loop of zero energy states where the two bands touch.

### III. WEYL NODAL LOOP

#### A. Model Hamiltonian

In this section, we delve into the fundamental characteristics of the Weyl Nodal Loop (WNL) model as introduced in [1]. Specifically, we investigate a two-band model of a WNL system situated on a cubic lattice affected by short-range disorder. The Hamiltonian describing this system without any disorder is:

$$H = \sum_k c_k^\dagger H_k c_k \quad (11)$$

$$= \sum_k c_k^\dagger ([t_x \cos k_x + t_y \cos k_y + \cos(k_z) - m] \tau_x + [t_2 \sin k_z] \tau_y) c_k$$

$\tau_x, \tau_y$  are the Pauli matrices and  $c_k^\dagger(c_k)$  is the creation (annihilation) operator in momentum space. The eigenvalue of the Hamiltonian is

$$E(\vec{k}) = \pm |t_x \cos k_x + t_y \cos k_y + \cos(k_z) - m + it_2 \sin k_z|$$

For a certain choice of  $(t_x, t_y, t_2, m)$ , it is possible to obtain a single nodal line (figure 2). We will get a nodal line set of parameters:  $k_z = 0$  and  $t_x \cos k_x + t_y \cos k_y + 1 - m = 0$ .

To gain an intuitive understanding of the lattice structure and visualize how electron hops between points (Figure 3), we require a real-space representation. This can be achieved by performing an inverse Fourier transform in all directions, allowing us to obtain the real-space depiction of the nodal line Hamiltonian.

$$H = \frac{t_x}{2} \sum_i (a_i^\dagger b_{i+e_x} + a_i^\dagger b_{i-e_x}) + \frac{t_y}{2} \sum_i (a_i^\dagger b_{i+e_y} + a_i^\dagger b_{i-e_y}) + \frac{1}{2} \sum_i ((1-t_2) a_i^\dagger b_{i+e_z} + (1+t_2) a_i^\dagger b_{i-e_z}) - m a_i^\dagger b_i + h.c.$$

This real space picture is important to add the disorder to the system. After adding the disorder, the Hamiltonian will be

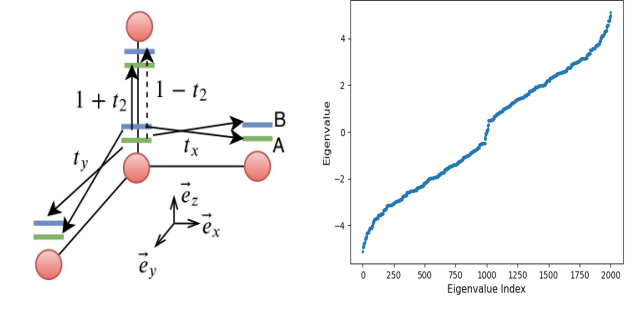


Figure 3. Left panel: The real space picture of the model Red circle is the lattice points, blue and green are two orbitals at each site [1]. Right panel: Eigenvalue in real space for linear system  $L = 10$  under PBC in all directions.

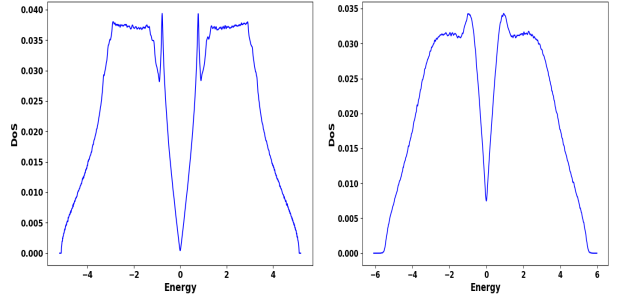


Figure 4. The DoS of the system with  $N_m = 1000$  and  $R = 1$  with  $W = 0$  (left panel) and  $W = 3.25$  (right panel)

nian will be

$$H = \sum_k c_k^\dagger H_k c_k + \sum_r c_r^\dagger V(r) c_r \quad (12)$$

The second term is the disorder potential, where  $r$  is a lattice site,  $\alpha$  is an orbital index and  $V(r) = \text{diag}(v_{r1}, v_{r2})$  with random variables  $v_{r\alpha} \in [-W/2, W/2]$ .

#### B. Density of State estimation

We employ the kernel polynomial method (KPM) with an expansion in Chebyshev polynomials up to order  $N_m$  [2-3] to numerically characterize the spectral function properties and compute the Density of States (DoS). Our calculations are conducted on systems with linear dimensions up to  $L = 160$  under periodic boundary conditions in each direction. As a semimetal, we anticipate a linear dispersion near the Dirac point or Fermi level, a characteristic that aligns with our observations in Figure 4. Additionally, we note that increasing the disorder strength leads to a jump in the density of states, resulting in a finite value at  $E = 0$ , as depicted in Figure 5.

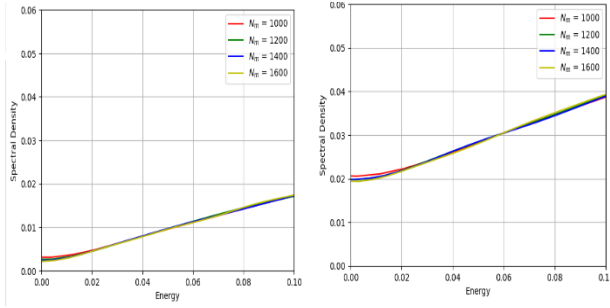


Figure 5. The DoS of the system  $E = 0$  with different  $N_m$  and  $R = 1$  with  $W = 2$  (left panel) and  $W = 3$  (right panel)

#### IV. CONCLUSION, DISCUSSION AND FUTURE DEVELOPMENTS

The main objective of the project was to utilize the Kernel Polynomial Method (KPM) for calculating the Density of States (DoS) of the Weyl Nodal loop. The first crucial step involved a mathematical derivation of KPM, laying the foundation for subsequent implementation. The numerical experiment section focused on applying these mathematical concepts in Python and running simulations on graphene, which demonstrated promising and accurate results in terms of DoS calculations. Notably, the KPM method showcased efficiency by achieving accuracy with relatively few random vectors, typically ranging from 10 to 30. Comparatively, it's essential to evaluate how KPM performs against other methods for computing DoS and related quantities [3]. Additionally, while the discussed algorithm is suitable for Hermitian systems, exploring methods for finding DoS in Non-Hermitian systems remains unexplored, offering insights into unique properties like the skin effect in topology [10].

Future work may involve extending this method to compute the expectation value of specific operators or exploring time dynamics beyond the Hermitian limit. This project is a foundational step towards addressing such research questions and potentially unlocking new insights into complex system behaviours.

#### V. SUPPLEMENTARY INFORMATION

##### A. Density of States

The density of states is an essential parameter in characterizing a system before conducting any measurements or probing. It provides crucial insights into the distribution of energy states within the system, particularly at the eigenvalues  $E_k$  corresponding to the eigenvectors  $|k_i\rangle$  of the Hamiltonian  $H$ . The density

of states, denoted as  $\rho(E_k)$ , represents the number of energy states between  $E$  and  $E + dE$  in a system [6, 7]. If the eigenvectors  $|k_i\rangle$  of the Hamiltonian  $H$  (with dimension  $D^2$ ) correspond to the eigenstates and  $E_k$  are the eigenvalues, then the density of states can be expressed as:

$$\rho(E_k) = \frac{1}{D} \delta(E - E_k) \quad (13)$$

Understanding the density of states is not just about counting states but also relates to the expectation value of an operator  $\hat{O}$ .

$$\langle \hat{O} \rangle = \int \rho(E) O(E) dE \quad (14)$$

Here,  $O(E)$  represents the operator's spectral density. This computation allows us to glean valuable information about the system's behavior and properties without directly probing it, aiding in theoretical analyses and predictions.

##### B. Chebyshev polynomial

There is a polynomial structure of  $\cos(n\theta)$  and  $\sin(n\theta)$ . From this, we define

$$T_n(\cos \theta) = \cos(n\theta)$$

$$\implies T_n(x) = \cos(n \arccos(x)) \quad (15)$$

which is known as the **Chebyshev polynomial of 1st kind** [figure 6]. Similarly, we can define the

$$U_n(\cos \theta) = \frac{\sin((n+1)\theta)}{\sin \theta}$$

$$\implies U_n(x) = \frac{\sin((n+1) \arccos(x))}{\sin(\arccos(x))} \quad (16)$$

This is known as **Chebyshev polynomial of 2nd kind**. We will mostly restrict ourselves to our project's 1st kind of polynomial as it's more stable and converges very well. So, let's discuss some important relations of 1st kind of polynomials.

##### Recurrence Relation:

The recurrence relation of 1st kind Chebyshev polynomials are as follows

$$\begin{aligned} & T_{m+n}(\cos \theta) + T_{m-n}(\cos \theta) \\ &= \cos((m+n)\theta) + \cos((m-n)\theta) \\ &= \cos(m\theta) \cos(n\theta) - \sin(m\theta) \sin(n\theta) \\ &+ \cos(m\theta) \cos(-n\theta) - \sin(m\theta) \sin(-n\theta) \\ &= 2 \cos(m\theta) \cos(n\theta) \\ &= 2T_m(\cos \theta) T_n(\cos \theta) \end{aligned}$$

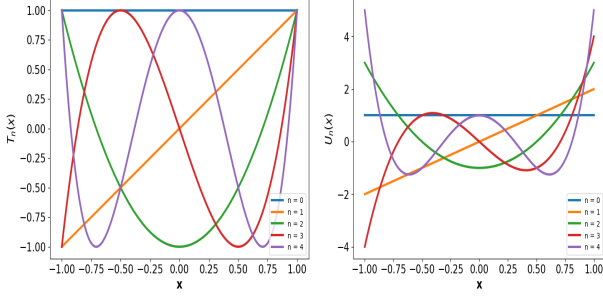


Figure 6. Chebyshev Polynomial of 1st and 2nd kind for first five order

Similarly, we can derive another useful recurrence relation

$$\begin{aligned} T_{m+n}(\cos \theta) - T_{m-n}(\cos \theta) \\ = 2(x^2 - 1)U_{m-1}(\cos \theta)U_{n-1}(\cos \theta) \end{aligned}$$

**Orthogonality condition:** The orthogonality condition is as follows

$$\begin{aligned} \int_{-1}^{-1} \frac{T_m(x)T_n(x)}{\pi\sqrt{1-x^2}} dx &= \int_{\pi}^0 \frac{T_m(\cos \theta)T_n(\cos \theta)}{\pi\sqrt{1-\cos^2 \theta}} (-\sin \theta d\theta) \\ &= \int_0^{\pi} \frac{\cos(n\theta)\cos(m\theta)}{\pi\sqrt{1-\cos^2 \theta}} d\theta \\ &= \left(\frac{\delta_{n,0}+1}{2}\right)\delta_{m,n} \end{aligned}$$

**Functional expansion:** Given a positive weight function  $w(x)$  defined on the interval  $[a, b]$  we can introduce a scalar product between two integrable functions  $f, g : [a, b] \rightarrow \mathbb{R}$ .

$$\langle f|g \rangle = \int_a^b w(x)f(x)g(x) dx \quad (17)$$

With respect to each such scalar product, there exists a complete set of polynomials  $p_n(x)$ , which fulfill the orthogonality relations

$$\langle p_n|p_m \rangle = \frac{\delta_{m,n}}{h_n} = \frac{\delta_{m,n}}{\langle p_n|p_n \rangle}$$

These orthogonality relations allow for an easy expansion of a given function  $f(x)$  in terms of the  $p_n(x)$ . In general, all types of orthogonal polynomials can be used for such an expansion [3, 2, 5].

Here our orthogonal and complete polynomial is  $T_n(x)$ . Therefore, we can write

$$f(x) = \sum_{n=0}^{\infty} \alpha_n T_n(x) = \sum_{n=0}^{\infty} \frac{\langle T_n|f \rangle}{\langle T_n|T_n \rangle} T_n(x) \quad (18)$$

Now define a new orthogonal function  $\phi_n(x) = \frac{T_n(x)}{\pi\sqrt{1-x^2}}$ . As these  $\phi_n$  span the entire space and so a function  $f(x)$  can also be written as:

$$f(x) = \sum_{n=0}^{\infty} \frac{\langle \phi_n|f \rangle}{\langle \phi_n|\phi_n \rangle} \phi_n(x)$$

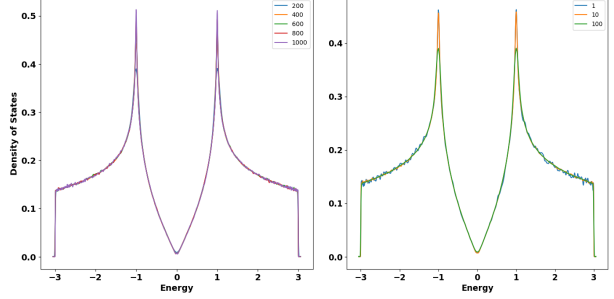


Figure 7. DoS of graphene by varying number of (Left panel) moments and (Right panel) random vector with  $r = 250$  in Kwant

$$= \langle \phi_0|f \rangle \phi_0(x) + 2 \sum_{n=1}^{\infty} \langle \phi_n|f \rangle \phi_n(x)$$

$$= \langle \phi_0|f \rangle \frac{T_0(x)}{\pi\sqrt{1-x^2}} + 2 \sum_{n=1}^{\infty} \langle \phi_n|f \rangle \frac{T_n(x)}{\pi\sqrt{1-x^2}}$$

$$= \frac{1}{\pi\sqrt{1-x^2}} (\mu_0 + 2 \sum_{n=1}^{\infty} \mu_n T_n(x))$$

Where  $\mu_n = \int_{-1}^1 f(x)T_n(x) dx$  is known as  $n$ th moment. This result is very useful since now the  $\alpha_n$  are modified to  $\mu_n$ , so to calculate these  $\mu_n$ , the weight function no longer has to be integrated.

### C. Numerical experiment

This section presents numerical outcomes from the Kernel Polynomial Method, highlighting the significance of the Kwant package [8]. For smaller system sizes, computing all Hamiltonian eigenstates  $|k_i\rangle$  yields exact results, enabling a comparison between KPM approximations and exact trace calculations. Key parameters for KPM include the number of moments ( $N$ ) and random vectors ( $R$ ), which are crucial for determining the energy points' resolution in the spectrum ( $K$ ).

To do a numerical estimation, we choose a Hexagonal Lattice (graphene) for computing DoS (figure - 7), which has recently been of great interest because of its intriguing physical properties, including the quantum Hall effect, superconductivity, etc. We choose the nearest neighbour hopping with hopping amplitude 1 and zero onsite potential.

We can see that for a small number of moments or random vectors, there is more function, and after increasing this to a certain number, the function dies, and DoS converges smoothly.

## VI. ACKNOWLEDGEMENT

I sincerely thank Dr. Kush Saha, my supervisor, for entrusting me with the opportunity to delve into this fascinating numerical technique. I am equally grateful to Dr. Subhasis Basak, our course instructor, for incorporating this project into the curriculum and providing me with a rich learning experience. Additionally, I acknowledge PhD student Mr Ivan Dutta and my friend Aritra for their insightful discussions on KPM and invaluable assistance in crafting the WNL semimetal code, respectively.

## VII. REFERENCES

1. Miguel Goncalves, Pedro Ribeiro, Eduardo V. Castro, Miguel A. N. Araujo, *Disorder-Driven Multifractality Transition in Weyl Nodal Loops*, Physical Review Letters 124, 136405 (2020)
2. Roeland ter Hoeven, *The Kernel Polynomial Method applied to tight binding systems with time-dependence*, Bachelor Thesis, 2016
3. Alexander Weibe, Gerhard Wellein, Andreas Alvermann and Holger Fehske, *The kernel polynomial method*, Reviews of Modern Physics, Volume 78, January 2006
4. Koji Kobayashi, Tomi Ohtsuki, Ken-Ichiro Imura, and Igor F. Herbut, *Density of States Scaling at the Semimetal to Metal Transition in Three Dimensional Topological Insulators*, Physical Review Letters 1112, 016402 (2014)
5. Jose Hugo Garcia Aguilar, *The kernel polynomial method for quantum transport in disordered systems*, PhD Thesis, 2015
6. Ashcroft and Mermin, *Solid State Physics*, Saunders College Publishing, (1976)
7. Charles Kittel, *Introduction to Solid State Physics*, Wiley publication, (2005)
8. C. W. Groth, M. Wimmer, A. R. Akhmerov, X. Waintal, *Kwant: a software package for quantum transport*, New J. Phys. 16, 063065 (2014).
9. João Santos Silva, *Topology and Disorder in Nodal Loop Semimetals*, Master's thesis, 2021.
10. Ayan Banerjee, Ronika Sarkar, Soumi Dey and Awadhesh Narayan, *Non-Hermitian topological phases: principles and prospects*, J. Phys. : Condens. Matter 35 (2023)
11. All the codes for this project can be found in Numerical-Exp.ipynb and Weyl-Final.ipynb files.